

# A Fast Spectral Solver for the Heat Equation, with Applications to Navier–Stokes

David Darrow\*

Advisors: Alex Townsend<sup>†</sup>, Grady Wright<sup>‡</sup>

June 13, 2022

**Abstract.** We develop a spectral method to solve the heat equation in a closed cylinder, achieving a near-optimal  $\mathcal{O}(N \log N)$  complexity and high-order, *spectral* accuracy. The algorithm relies on a novel Chebyshev–Chebyshev–Fourier (CCF) discretization of the cylinder, which is easily implemented and decouples the heat equation into a collection of smaller, sparse Sylvester equations. In turn, each of these equations is solved using the alternating direction implicit (ADI) method, which improves the complexity of each solve from cubic in the matrix size (in more traditional methods) to log-linear; overall, this represents an improvement in the heat equation solver from  $\mathcal{O}(N^{7/3})$  (in traditional methods) to  $\mathcal{O}(N \log N)$ . Lastly, we provide numerical simulations demonstrating significant speed-ups over traditional spectral collocation methods and finite difference methods, and we provide a framework by which this heat equation solver could be applied to the incompressible Navier–Stokes equations. For the latter, we decompose the equations using a poloidal–toroidal (PT) decomposition, turning them into heat equations with nonlinear forcing from the advection term; by using implicit–explicit methods to integrate these, we can achieve the same  $\mathcal{O}(N \log N)$  complexity and spectral accuracy achieved here in the heat equation.

---

\*Massachusetts Institute of Technology, Department of Mathematics

<sup>†</sup>Cornell University, Department of Mathematics

<sup>‡</sup>Boise State University, Department of Mathematics

**1. Introduction.** The forced heat equation models the diffusion of heat through a homogeneous, isotropic medium; it is given by

$$(\partial_t - \alpha \nabla^2)T = g(x, t),$$

where  $T$  is the local temperature field,  $\alpha$  is the thermal diffusivity of the medium, and  $g$  is the rate of heat generation. More than just heat diffusion, however, the heat equation provides an archetype for diffusion problems in general contexts—for one, viscous or slow-moving (incompressible) fluids obey the *Stokes* equations, a diffusive approximation to the general Navier–Stokes equations when viscous forces dominate the flow:

$$\nabla \cdot \vec{v} = 0, \quad (\partial_t - \frac{1}{Re} \nabla^2) \vec{v} = -\vec{v} \cdot \nabla \vec{v} - \rho^{-1} \nabla p \approx -\rho^{-1} \nabla p.$$

Here,  $\vec{v}$  is the fluid velocity,  $p/\rho$  is the normalized fluid pressure, and  $Re$  is the *Reynolds number* of the flow, a dimensionless group characterizing the relative effects of advective and viscous forces; in making the Stokes approximation, we are assuming  $Re \ll 1$ .

As such, the heat equation has seen a great deal of attention in both numerical analysis and in industry applications. For one, finite difference (FD) methods for the heat equation are well-catalogued in textbooks (see [Coo12] for a modern introduction), and for good reason; FD approaches are *spatially local*, meaning that (a) they can be more easily adapted to new geometries and (b) they allow for equation coefficients (such as the thermal diffusivity) to vary in space. For more recent examples, Berrone has adapted the *finite element* (FE) method to systems with discontinuous coefficients [Ber09], and Causley et al. have introduced a powerful convolution-based approach to solve the heat equation and certain nonlinear analogues in optimal time [CCCS16].

Though these approaches allow for fast solvers and great flexibility in the form of the equation and domain, they trade for this by giving only *polynomial* accuracy in the solution itself—that is, the solution generally carries an error of  $\mathcal{O}(N^{-M})$ , where  $N$  is the discretization lattice size and  $M$  is a small positive integer [LeV07]. To achieve better resolution, high-order *spectral collocation methods* are often applied; these approximate the solution space using degree- $N$  polynomials, allowing for far better,  $\mathcal{O}(\rho^{-N})$  errors (for some  $\rho > 1$ ), but traditionally at the cost of more expensive runtimes [Tre19]. Spectral *coefficient* methods circumvent these runtimes in certain cases, but only when derivatives can be expressed as sparse matrices in the chosen basis [Boy00]; in practice, this means they are particularly suited for periodic domains, where the standard Fourier basis diagonalizes differentiation.

More recently, by leveraging properties of ultraspherical polynomials, Olver and Townsend introduced a coefficient-based (rather than collocation) spectral method

that allows for well-conditioned and near-optimal time ODE solvers in closed domains, even with spatially-varying coefficients [OT13]. This method has more recently been adapted to higher dimensions in highly symmetric domains, namely, the disk and sphere [WTW17] and the unit ball [BT20]. Notably, an earlier work by Torres and Coutsias [TC99] was able to achieve near-optimal complexity in solving the incompressible Navier–Stokes equations on the disk by employing a post-conditioned Chebyshev- $\tau$  method [Boy00], but we utilize the ultraspherical method due to its flexibility and relative ease of implementation. Independently, a wide variety of fast spectral methods has been developed to solve PDEs in various settings [BVO<sup>+</sup>20, SK21].

In this paper, we adapt the methods of Olver and Townsend to the closed cylinder, achieving a near-optimal complexity solver for the heat equation with spectral accuracy. To do so, we overcome a key obstacle unique to the cylinder; where the disk, sphere, and unit ball have only *one* spatial dimension approximated by Chebyshev polynomials (and the rest by Fourier series), the cylinder has two: the  $r$  and  $z$  directions. As a result, for each Fourier mode, we must solve a sparse Sylvester equation rather than a system of linear equations. For this, we apply the alternating direction implicit (ADI) method of [PR55], resulting in overall  $\mathcal{O}(N \log N)$  time (as compared to the  $\mathcal{O}(N^{7/3})$  necessary to solve these equations directly).

To integrate the heat equation forward in time, we use a high order *backwards differentiation formula* (BDF) [CH52]. This allows for a high degree of accuracy in time, while maintaining stability; in particular, as the heat equation is *stiff*, implicit methods (such as BDF) are necessary for its solution.

Secondly, we demonstrate a potential application of this method to solve the Navier–Stokes equations in the cylinder, with the same time and accuracy as with the heat equation. Turbulence modeling highlights the benefits of our approach; the increased digits of precision with spectral accuracy—often 5–10 or more—are essential for turbulence resolution [Zhi15].

To solve the Navier–Stokes equations, we introduce the poloidal–toroidal (PT) decomposition to split incompressible vector fields into two scalar components each. The new variables allow for parallelization and avoid projection methods to maintain the incompressibility of the fluid, though an alternate approach using projection methods was introduced first in [LS98]. The PT decomposition can be found by solving two Poisson equations, which—using our developed method for the heat equation—does not increase the computational complexity of  $\mathcal{O}(N \log N)$  operations per time step. At this point, the Navier–Stokes equations are decomposed into independent equations on poloidal and toroidal fields, which can be solved similarly to a set of two scalar heat equations (with non-linear forcing).

Instead of BDF, which is no longer feasible for a nonlinear equation, we apply implicit–explicit versions of these formulas, following [ARW95]. These integrate the diffusive, linear component as before, but now integrate the nonlinear components of

the Navier–Stokes equations explicitly.

Notably, along the way, we develop a method to solve the Poisson and Helmholtz equations in the closed cylinder—most generally, equations of the following form:

$$(k^2 - \alpha \nabla^2)T = g(x, t),$$

where  $k$  can be either zero or nonzero. These equations follow from the PT decomposition and our time-discretization of the heat equation, respectively, and arise in physical applications ranging from electrostatics to quantum mechanics.

Our domain of interest for this paper is the closed cylinder in  $\mathbb{R}^3$ , though the method can be generalized to other polar or spherical geometries. The cylinder has many applications throughout the sciences, including studying blood flow, storing fuel in rockets, and understanding properties of hurricanes. Accordingly, the cylindrical coordinates  $(r, z, \theta)$  are used throughout. Note that this geometry differs from studying a flow across a cylinder, a problem common in aerodynamics.

Our code was originally developed as part of MIT PRIMES 2017, and is freely available on GitHub [Dar17]; since then, these methods have been adapted for fast simulations of active fluids in a ball [BDST21] and to develop improved Poisson solvers in various geometries [FT19].

**Acknowledgments.** I would like to thank Professors Alex Townsend (Cornell) and Grady Wright (Boise State University), who suggested the original problem and mentored me throughout this entire process. I would also like to thank the MIT PRIMES research program, and particularly Professor Pavel Etingof, Dr. Tanya Khovanova, and Dr. Slava Gerovitch for making this research possible.

**2. Spectral Approximation of Functions in the Cylinder.** In order to approximate solutions to the heat equation in the cylinder, we first discretize the system by only enforcing the equations at  $N$  selected *discretization points*. Instead of working with all functions, the discretized system is restricted to a certain  $N$ -dimensional space of high order polynomials on the cylinder. This approach, a *spectral method*, provides one unique advantage over current methods: so-called *spectral accuracy*.

While standard simulation methods achieve algebraic accuracy—errors of  $\mathcal{O}(N^{-k})$  for some  $k$  [LeV07]—spectral accuracy achieves errors of  $\mathcal{O}(\rho^{-N})$  for some  $\rho > 1$ . Even when  $N$  is as small as 1000, this often represents an improvement over algebraically accurate methods of several orders of magnitude. This accuracy is also uniform throughout the cylinder; some current methods, such as *finite element methods*, underresolve the boundary of the region, potentially missing important effects of “wall-bounded turbulence” [Kra79].

Let  $C \subset \mathbb{R}^3$  be the closed cylinder written in cylindrical coordinates  $(r, z, \theta)$ , where  $-1 \leq r \leq 1$ ,  $-\pi \leq \theta \leq \pi$ , and  $-1 \leq z \leq 1$ . Let  $m, n, p \in \mathbb{N}$  be the number of discretization points in the radial, vertical, and angular directions, respectively. The

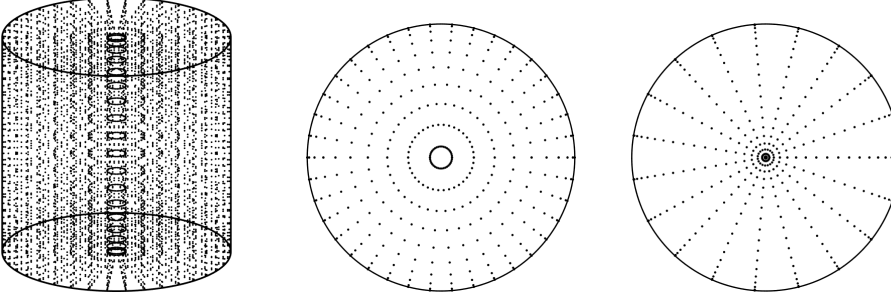


Fig. 2.1: Illustration of the  $\text{CCF}_{(m,n,p)}$  discretization grid (along with a cross-section), for  $m = n = p = 20$ , contrasted with the corresponding undoubled grid (the current paradigm). Unlike the “undoubled” grid on the right,  $\text{CCF}_{(m,n,p)}$  does not cluster the majority of the points near the centerline of the cylinder.

total number of discretization points in  $C$  is then  $N = mnp$ .

DEFINITION 2.1. *The doubled  $m \times n \times p$  Chebyshev–Chebyshev–Fourier grid, denoted by  $\text{CCF}_{(m,n,p)}$ , is the set (in cylindrical coordinates  $(r, z, \theta)$ ) of points  $\mathbf{x}_{(j,k,\ell)}$ , where*

$$\mathbf{x}_{(j,k,\ell)} = \left( \cos \left( \frac{(m-j-1)\pi}{m-1} \right), \cos \left( \frac{(n-j-1)\pi}{n-1} \right), \frac{(2\ell-p)\pi}{p} \right),$$

$$j, k, \ell \in \mathbb{Z}, \quad 0 \leq j < m, \quad 0 \leq k < n, \quad 0 \leq \ell < p.$$

This “doubled” grid, shown in Figure 2.1, can be contrasted with the non-doubled Chebyshev–Chebyshev–Fourier grid in the cylinder, which chooses the radial Chebyshev points between 0 and 1. This clusters discretization points near the azimuth (centerline) of the cylinder: a full third of the points are within the center area  $1/16^{\text{th}}$  the cross sectional size of the region, slowing down computation significantly without providing an increase in approximation accuracy. The doubled grid, however, chooses the radial Chebyshev points between  $-1$  and  $1$ . This grid is an improvement over the standard one; it distributes points almost evenly with respect to cross sectional area.

Now, we must choose some  $N$ -dimensional basis to span the set of functions restricted to our discretization grid. As it turns out, the set of “ $\text{CCF}_{(m,n,p)}$  polynomials”, defined below, does the trick; the set satisfies necessary existence and uniqueness theorems, allows easy representation of certain differential operators, and interpolates with high accuracy [Tre19].

DEFINITION 2.2. *A  $\text{CCF}_{(m,n,p)}$  polynomial is a function  $q_{(j,k,\ell)} : C \rightarrow \mathbb{R}^3$  of the following form:*

$$q_{(j,k,\ell)}(r, z, \theta) = T_j(r)T_k(z)e^{i(\ell - \lfloor p/2 \rfloor)\theta},$$

where  $T_K$  is the degree  $K$  Chebyshev polynomial of the first kind and  $j, k, \ell$  have the same bounds as in Definition 2.1. The complex vector space spanned by these

$CCF_{(m,n,p)}$  polynomials is denoted  $P_{(m,n,p)}$ .

Also of use are these two sorts of polynomials:  $U_K = C_K^{(1)}$  indicates the degree  $K$  Chebyshev polynomial of the second kind, and  $C_K^{(2)}$  indicates the degree  $K$  ultraspherical polynomial such that the set  $\{C_i^{(2)}\}_{i=0}^\infty$  is orthogonal with respect to the weight  $(1-x^2)^{3/2}$  on  $[-1, 1]$ .

Any continuous function  $f : C \rightarrow \mathbb{R}$  has a unique interpolant  $f^* \in P_{(m,n,p)}$ , i.e.  $f = f^*$  on  $CCF_{(m,n,p)}$ . This interpolant is of the form

$$f^*(r, z, \theta) = \sum_{j=0}^{m-1} \sum_{k=0}^{n-1} \sum_{\ell=0}^{p-1} f^{(j,k,\ell)} T_j(r) T_k(z) e^{i(\ell - \lfloor p/2 \rfloor)\theta}.$$

In order to find the coefficients  $f^{(j,k,\ell)}$ , start with the set of values of  $f$  on the grid:  $f_{(j,k,\ell)} = f(\mathbf{x}_{(j,k,\ell)})$ . Perform the discrete cosine transform of type I (DCT) first on each  $m$ -tuple  $(f_{(j,k,\ell)})_{j=0}^{m-1}$ , so that  $(f_{(k,\ell)}^{(j)})_{j=0}^{m-1} = \text{DCT}(f_{(j,k,\ell)})_{j=0}^{m-1}$ , for all  $k, \ell$ . Then, perform another DCT, but this time on the  $n$ -tuple  $(f_{(k,\ell)}^{(j)})_{k=0}^{n-1}$ , so that  $(f_{(\ell)}^{(j,k)})_{k=0}^{n-1} = \text{DCT}(f_{(k,\ell)}^{(j)})_{k=0}^{n-1}$ , for all  $j, \ell$ . Finally, perform a discrete Fourier transform (DFT) on the  $p$ -tuple  $(f_{(\ell)}^{(j,k)})_{\ell=0}^{p-1}$ , so that  $(f^{(j,k,\ell)})_{\ell=0}^{p-1} = \text{DFT}(f_{(\ell)}^{(j,k)})_{\ell=0}^{p-1}$ , for all  $j, k$ . Each value  $f^{(j,k,\ell)}$  is then the coefficient on the basis function  $q_{(j,k,\ell)}$ . This series of transforms can be performed in  $\mathcal{O}(N \log N)$  operations with the Fast Fourier Transform, where  $N = mnp$ .

**3. The Heat Equation.** The heat equation in  $C$  is as follows:

$$\left( \frac{\partial}{\partial t} - \alpha \nabla^2 \right) T = g(r, z, \theta, t),$$

where  $T(r, z, \theta, t)$  denotes the temperature at a given point in space and time in the cylinder,  $g(r, z, \theta, t)$  is the rate of heat generation at a point  $(r, z, \theta)$  at time  $t$ , and  $\alpha > 0$  is the “thermal diffusivity” of the domain, or the rate at which heat transfers to colder areas.

To solve the heat equation, we use the  $b^{th}$ -order backwards differentiation formula (BDF), given below for  $b = 1, 4$  with time-step  $h$ :

*BDF 1.*

$$f(t+h) - h \frac{d}{d\tau} f(\tau)|_{\tau=t+h} = f(t) + \mathcal{O}(h^2),$$

*BDF 4.*

$$f(t+h) - \frac{12}{25} h \frac{d}{d\tau} f(\tau)|_{\tau=t+h} = \frac{48}{25} f(t) - \frac{36}{25} f(t-h) + \frac{16}{25} f(t-2h) - \frac{3}{25} f(t-3h) + \mathcal{O}(h^5).$$

Define  $\delta^{(b)} f(t)$  to be the RHS of the  $b^{th}$  order BDF (with the  $\mathcal{O}(h^K)$  term omit-

ted), and define  $\kappa^{(b)}$  to be the (positive) coefficient of  $\frac{d}{d\tau}f(\tau)$  in the same equation. For instance,  $\kappa^{(4)} = \frac{12}{25}h$  and  $\delta^{(4)}f(t) = \frac{48}{25}f(t) - \frac{36}{25}f(t-h) + \frac{16}{25}f(t-2h) - \frac{3}{25}f(t-3h)$ . We can work this approximation into the heat equation by solving the latter for  $\frac{\partial}{\partial t}T$ :

$$(3.1) \quad \frac{\partial}{\partial \tau}T(r, z, \theta, \tau)|_{\tau=t+h} \approx \alpha \nabla^2 T(r, z, \theta, t+h) + g(r, z, \theta, t+h).$$

Once we know  $\delta^{(b)}f(t)$ , which we would if we were progressing through equidistant time steps, we can plug (3.1) into the  $b^{th}$  order BDF and get a *Helmholtz equation*:

$$(I - \kappa^{(b)}\alpha \nabla^2) T(r, z, \theta, t+h) \approx \delta^{(b)}T(r, z, \theta, t) + \kappa^{(b)}g(r, z, \theta, t+h),$$

where the RHS is already known and  $I$  is the identity operator. An initial problem is in the apparent unboundedness of the operator on the LHS at  $r = 0$ , as it includes the terms  $\frac{1}{r}$  and  $\frac{1}{r^2}$ :

$$I - \kappa^{(b)}\alpha \nabla^2 = I - \kappa^{(b)}\alpha \left( \frac{1}{r} \frac{\partial}{\partial r} + \frac{\partial^2}{\partial r^2} + \frac{1}{r^2} \frac{\partial^2}{\partial \theta^2} + \frac{\partial^2}{\partial z^2} \right).$$

To resolve this, we multiply both sides of the Helmholtz equation by  $r^2$  to obtain

$$(3.2) \quad r^2 (I - \kappa^{(b)}\alpha \nabla^2) T(r, z, \theta, t+h) \approx r^2 \delta^{(b)}T(r, z, \theta, t) + \kappa^{(b)}r^2 g(r, z, \theta, t+h).$$

The  $\text{CCF}_{(m,n,p)}$  polynomial basis provides significant benefits for solving the above equation. If we work in “coefficient space”, or the set of coefficients  $(T^{(j,k,\ell)})$ , then this  $T(r, z, \theta, t+h)$  can be found in near-optimal time and with spectral accuracy.

We can “discretize” the left-hand operator in equation (3.2) in the space  $P_{(m,n,p)}$ . To start with, the  $m \times n$  matrix  $\mathbf{X}_\ell(t)$  is defined by  $[\mathbf{X}_\ell(t)]_{j,k} = T^{(j,k,\ell)}(t)$ , where  $[\mathbf{X}_\ell(t)]_{j,k}$  is the element in the  $j^{th}$  row and  $k^{th}$  column of  $\mathbf{X}_\ell(t)$ . We similarly define the  $m \times n$  matrix  $\mathbf{g}_\ell(t)$  as the matrix of interpolation coefficients of  $g(r, z, \theta, t)$ .

From here, we discretize necessary operators as matrices to act on  $\mathbf{X}_\ell(t)$ .

- The matrix  $C_{01}$ , which converts a  $T_i$  coefficient vector to a  $U_i$  coefficient vector; and the matrix  $C_{12}$ , which converts a  $U_i \equiv C_i^{(1)}$  coefficient vector to a  $C_i^{(2)}$  coefficient vector:

$$C_{01} = \begin{bmatrix} 0 & \frac{1}{2} & & & \\ \frac{1}{2} & 0 & \frac{1}{2} & & \\ & \frac{1}{2} & \ddots & \ddots & \\ & & \ddots & \ddots & \frac{1}{2} \\ & & & \frac{1}{2} & 0 \end{bmatrix}, \quad C_{12} = \begin{bmatrix} 1 & 0 & -\frac{1}{3} & & \\ & \frac{1}{2} & 0 & \ddots & \\ & & \frac{1}{3} & \ddots & -\frac{1}{n} \\ & & & \ddots & 0 \\ & & & & \frac{1}{n} \end{bmatrix}.$$

The matrix  $C_{02}$  is defined by  $C_{02} = C_{12}C_{01}$ . It converts a  $T_i$  coefficient vector to a  $C_i^{(2)}$  coefficient vector.

- The  $b^{th}$ -order BDF operator  $\delta^{(b)}$  is found by sampling its argument at  $(t, t - h, \dots, t - (b - 1)h)$  and taking differences, as with the RHS of the  $b^{th}$  order BDF. For instance,

$$\delta^{(4)}\mathbf{X}_\ell(t) = \frac{48}{25}\mathbf{X}_\ell(t) - \frac{36}{25}\mathbf{X}_\ell(t - h) + \frac{16}{25}\mathbf{X}_\ell(t - 2h) - \frac{3}{25}\mathbf{X}_\ell(t - 3h).$$

- The multiplication operator  $R$ , which multiplies a  $C_k^{(2)}(r)$  coefficient vector by  $r$ :

$$R = \begin{bmatrix} 0 & \frac{2}{3} & & & \\ \frac{1}{4} & 0 & \frac{5}{8} & & \\ & \frac{1}{3} & 0 & \ddots & \\ & & \ddots & \ddots & \frac{n+2}{2n+2} \\ & & & \frac{n-1}{2n} & 0 \end{bmatrix}.$$

Note that the subdiagonal pattern starts with  $\frac{2-1}{4} = \frac{1}{4}$ , not with  $\frac{1-1}{2} = 0$ . For convenience, also define  $R_2 = R^2 C_{02}$ .

- The differentiation operator  $D_1 = C_{01} \frac{\partial}{\partial r}$ , where  $\frac{\partial}{\partial r}$  differentiates a  $T_k(r)$  coefficient vector by  $r$ ; and the second differentiation operator  $D_2 = C_{02} \frac{\partial^2}{\partial r^2}$ , where  $\frac{\partial^2}{\partial r^2}$  differentiates a  $T_k(r)$  coefficient vector twice by  $r$ :

$$D_1 = \begin{bmatrix} 0 & 1 & & & \\ & & 2 & & \\ & & & \ddots & \\ & & & & n-1 \\ & & & & 0 \end{bmatrix}, \quad D_2 = \begin{bmatrix} 0 & 0 & 4 & & \\ & & & \ddots & \\ & & & & 2n-2 \\ & & & & 0 \\ & & & & 0 \end{bmatrix}.$$

With these operators, equation (3.2) can be discretized (with the extrapolation  $g(t + h) \approx g(t)$ ) as the following matrix equation:

$$(3.3) \quad \left( R_2 - \kappa^{(b)} \alpha (RC_{12}D_1 + R^2D_2 - \ell^2 C_{02}) \right) \mathbf{X}_\ell(t + h) C_{02}^T - \kappa^{(b)} \alpha R_2 \mathbf{X}_\ell(t + h) D_2^T = R_2 \left( \delta^{(b)} \mathbf{X}_\ell(t) + \kappa^{(b)} \mathbf{g}_\ell(t) \right) C_{02}^T.$$

The discretization process used above is discussed further in [OT13]. There are two notable properties of equation (3.3): each value of  $\ell$  can be solved for independently (we can “decouple in  $\theta$ ”), and every matrix used in the construction of the equation is very sparse. We use the ADI method to solve equation (3.3) in  $\mathcal{O}(N \log N)$  operations [PR55].

ALGORITHM 1 (ADI Method). *Let  $A, C$  be  $m \times m$  complex matrices,  $B, D$  be  $n \times n$  complex matrices, and  $X, E$  be  $m \times n$  complex matrices. Set two complex-valued*



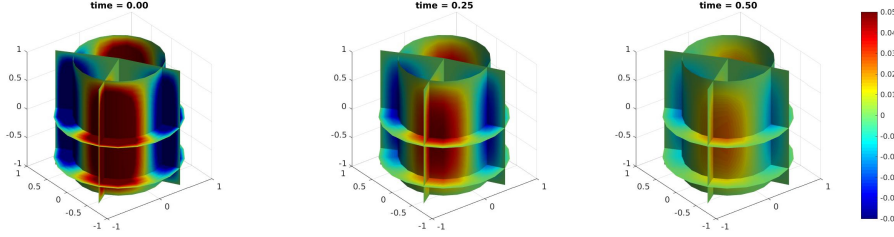


Fig. 3.1: A simulation of the heat equation in the cylinder  $C$ . This is shown on various slices of the cylinder, where the temperature value is given by the color bars on the right of each figure. There is no advective motion, making the heat equation computationally faster to solve than the Navier–Stokes equations.

sequences  $(u_k)_{k=0}^{K-1}$  and  $(v_k)_{k=0}^{K-1}$ , and set  $X_0 = 0$ .

The ADI method for approximately solving the Sylvester equation  $AXB + CXD = E$  for  $X$  is as follows:

1. Solve  $(u_k C - A)X_{k+\frac{1}{2}}B = CX_k(u_k B + D) + E$  for  $X_{k+\frac{1}{2}}$ .
2. Solve  $CX_{k+1}(v_k B + D) = (v_k C - A)X_{k+\frac{1}{2}}B - E$  for  $X_{k+1}$ .
3. Repeat steps 1 and 2 for  $K$  iterations;  $X_K \approx X$ .

With an appropriate choice of  $(u_k)_{k=0}^{K-1}$  and  $(v_k)_{k=0}^{K-1}$ , we can get sufficient accuracy with  $K = \mathcal{O}(\log mn)$ . This iteration then gives an accurate solution in  $\mathcal{O}(mn \log mn)$  operations, assuming that the initial Sylvester equation is well-conditioned. All such equations in this work are well-conditioned unless otherwise stated.

Equation (3.3) is of the sort required for the ADI algorithm; at each time step, we can solve for each  $\mathbf{X}_\ell$  in  $\mathcal{O}(mn \log mn)$  operations. There are  $p$  choices of  $\ell$ , though, so this is scaled up to  $\mathcal{O}(mnp \log mn)$  total operations at each time step. Since  $N = mnp$ , the final algorithm has a total of  $\mathcal{O}(N \log N)$  operations. This compares to times of  $\mathcal{O}(N^{7/3})$ , or  $\mathcal{O}(m^3 n^3 p)$ , with current spectral methods. A solution example is illustrated in Figure 3.1.

**4. The Poloidal–Toroidal Decomposition.** The *poloidal–toroidal decomposition* (PT decomposition) is a critical component for quickly and accurately solving the incompressible Navier–Stokes equations for two reasons. First, it allows these more complex vector equations to “decouple” into two scalar heat-like equations. We can maintain our spectral accuracy and near-optimal computation time from the heat equation solver, avoiding the large computational times faced by current solvers that work with the primitive form of the equations. Second, it ensures that the computed velocity field  $\vec{v}$  is exactly incompressible, whereas current solvers maintain this central property by projecting the velocity field after each time step, introducing potentially large errors in the simulation [She96].

Let  $\hat{z}$  be the unit vector in the direction of the azimuth (the “ $z$ -direction”) of  $C$ .

DEFINITION 4.1. *The (cylindrical) poloidal–toroidal decomposition, or “PT decomposition”, of an incompressible vector field  $\vec{V}$  is an expression of  $\vec{V}$  in terms of the sum of a toroidal field and a poloidal field. A toroidal vector field  $\mathbf{T}$  is one of the form  $\mathbf{T} = \nabla \times [\lambda \hat{z}]$ , where  $\lambda$  is a scalar field. A poloidal vector field  $\mathbf{P}$  is one of the form  $\mathbf{P} = \nabla \times \nabla \times [\gamma \hat{z}]$ , where  $\gamma$  is a scalar field.*

We prove the existence of the PT decomposition of a general incompressible vector field in the cylinder. A more general discussion of the PT decomposition is given in [BT07].

THEOREM 4.2. *Let  $\vec{V} : C \rightarrow \mathbb{R}^3$  be an arbitrary incompressible vector field on  $C$ , i.e.,  $\nabla \cdot \vec{V} = 0$ . Then  $\vec{V}$  can be decomposed as a sum of a toroidal and a poloidal field:*

$$(4.1) \quad \vec{V} = \nabla \times [\lambda \hat{z}] + \nabla \times \nabla \times [\gamma \hat{z}],$$

where  $\lambda$  and  $\gamma$  are real-valued functions on  $C$ .

*Proof.* Because  $\vec{V}$  is incompressible and  $C$  is bounded,  $\vec{V} = \nabla \times \vec{A}$  for some vector potential  $\vec{A}$ . It is then sufficient to show that  $\vec{A} = \lambda \hat{z} + \nabla \times [\gamma \hat{z}] + \nabla \beta$ , as  $\nabla \beta$  is annihilated by the curl operator. Form an orthonormal basis of  $\mathbb{R}^3$ ,  $(\hat{x}, \hat{y}, \hat{z})$ . Within this basis, it must be shown that there exist functions  $\lambda = \lambda(x, y, z)$ ,  $\gamma = \gamma(x, y, z)$ , and  $\beta = \beta(x, y, z)$  such that  $\vec{A} = (\beta_x + \gamma_y)\hat{x} + (\beta_y - \gamma_x)\hat{y} + (\beta_z + \lambda)\hat{z}$ . For any  $\vec{A}$ ,  $\lambda = \vec{A} \cdot \hat{z} - \beta_z$  solves our target equation, which leaves the system

$$\beta_x + \gamma_y = \vec{A} \cdot \hat{x}, \quad \beta_y - \gamma_x = \vec{A} \cdot \hat{y}.$$

Differentiate the former equation by  $x$  and the latter by  $y$ , retrieving two new equations from their sum and difference respectively:

$$\beta_{xx} + \beta_{yy} = A_x \cdot \hat{x} + A_y \cdot \hat{y}, \quad \gamma_{xx} + \gamma_{yy} = A_x \cdot \hat{x} - A_y \cdot \hat{y}.$$

Along with the conditions that our target equation and its derivatives hold at the boundary, both Poisson equations have solutions. Thus, there exist  $\lambda$  and  $\gamma$  that satisfy equation (4.1).  $\square$

The scalar fields in this decomposition are not generally unique, though the vector fields are. To decompose the Navier–Stokes equations, the PT decomposition is required for two distinct vector fields:  $\vec{\omega} = \nabla \times \vec{v}$  and  $\nabla \times (\vec{v} \times \vec{\omega})$ . The former field,  $\vec{\omega} = \nabla \times \vec{v}$ , is defined as the “vorticity” of the fluid, which gives the axis of rotation and rotational velocity of the fluid in the cylinder.

COROLLARY 4.3. *The following two equalities hold:*

$$(4.2) \quad \vec{\omega} \equiv \nabla \times \vec{v} = \nabla \times [\lambda_\omega \hat{z}] + \nabla \times \nabla \times [\gamma_\omega \hat{z}],$$

$$(4.3) \quad \nabla \times [\vec{v} \times \vec{\omega}] = \nabla \times [\lambda_a \hat{z}] + \nabla \times \nabla \times [\gamma_a \hat{z}].$$

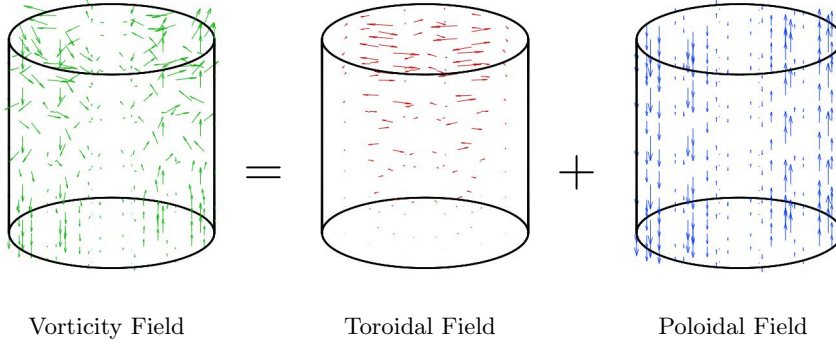


Fig. 4.1: An example of a vorticity vector field being decomposed into its poloidal and toroidal components. The components are each given by a single scalar field. The poloidal and toroidal fields were computed numerically.

*Proof.* As  $\vec{\omega} \equiv \nabla \times \vec{v}$  and  $\nabla \times (\vec{v} \times \vec{\omega})$  are both the curls of their respective vector potentials, the divergence operator annihilates both. Thus, they are both incompressible functions on  $C$ , and Theorem 4.2 says that a PT decomposition exists.  $\square$

Lastly, we need some fast and accurate method of *computing* the PT decomposition of an arbitrary vector field. Again, let  $\vec{V}$  be an arbitrary incompressible vector field, with its PT decomposition given by equation (4.1). Let  $\Delta_h = \partial_x^2 + \partial_y^2 = \frac{1}{r} \partial_r + \partial_r^2 + \frac{1}{r^2} \partial_\theta^2$ , in standard Cartesian and cylindrical coordinates respectively. This is the *horizontal Laplacian operator*, and takes the Laplacian as if its argument were only a function in two horizontal dimensions (at a given value of  $z$ ).

THEOREM 4.4. *With  $\vec{V}$ ,  $\gamma$ , and  $\lambda$  defined as in Theorem 4.2, then*

$$(4.4) \quad \hat{z} \cdot \vec{V} = -\Delta_h \gamma, \quad \hat{z} \cdot \nabla \times \vec{V} = -\Delta_h \lambda.$$

*Proof.* Form an orthonormal basis of  $\mathbb{R}^3$ ,  $(\hat{x}, \hat{y}, \hat{z})$ . Using the identity  $\hat{z} \cdot \nabla \times \vec{B} = \vec{B}_x \cdot \hat{y} - \vec{B}_y \cdot \hat{x}$ ,

$$\hat{z} \cdot \vec{V} = \hat{z} \cdot \nabla \times [\lambda \hat{z} + \nabla \times (\gamma \hat{z})] = (\hat{y} \cdot \partial_x - \hat{x} \cdot \partial_y)(\lambda \hat{z} + \nabla \times [\gamma \hat{z}]) = -\gamma_{xx} - \gamma_{yy} = -\Delta_h \gamma.$$

We perform the same calculation with  $\hat{z} \cdot \nabla \times \vec{V}$ . From direct calculation,  $\vec{V} \cdot \hat{x} = \lambda_y + \gamma_{xz}$  and  $\vec{V} \cdot \hat{y} = -\lambda_x + \gamma_{yz}$ , so

$$\hat{z} \cdot \nabla \times \vec{V} = (\hat{y} \cdot \partial_x - \hat{x} \cdot \partial_y) \vec{V} = -\lambda_{xx} + \gamma_{yzx} - \lambda_{yy} - \gamma_{xzy} = -\lambda_{xx} - \lambda_{yy} = -\Delta_h \lambda.$$

Just like we did with the heat equation, define the  $m \times n$  matrix  $\mathbf{\Lambda}_\ell$  [resp.  $\mathbf{\Gamma}_\ell$ ] by  $(\mathbf{\Lambda}_\ell)_{j,k} = \lambda^{(j,k,\ell)}$  [resp.  $(\mathbf{\Gamma}_\ell)_{j,k} = \gamma^{(j,k,\ell)}$ ], where  $(\lambda^{(j,k,\ell)})$  [resp.  $(\gamma^{(j,k,\ell)})$ ] are the interpolation coefficients for  $\lambda$  [resp.  $\gamma$ ] in  $\text{CCF}_{(n,m,p)}$ . Define  $\mathbf{V}_{r,\ell}$ ,  $\mathbf{V}_{\theta,\ell}$ , and  $\mathbf{V}_{z,\ell}$  similarly for the radial, angular, and vertical components of  $\vec{V}$  respectively. With the

same operators as before, the system (4.4) can be written as matrix equations:

$$(RC_{12}D_1 + R^2D_2 - \ell^2C_{02})\mathbf{\Lambda}_\ell = -R_2\mathbf{V}_{z,\ell},$$

$$(RC_{12}D_1 + R^2D_2 - \ell^2C_{02})\mathbf{\Gamma}_\ell = i\ell RC_{02}\mathbf{V}_{r,\ell} - (R^2C_{12}D_1 + RC_{02})\mathbf{V}_{\theta,\ell}.$$

These can be solved using the ADI method in  $\mathcal{O}(N \log N)$  operations. An example decomposition is shown in Figure 4.1.

**5. Rewriting the Navier–Stokes Equations.** We now have all of the tools at our disposal to rewrite the Navier–Stokes equations as a set of heat equations (with nonlinear forcing terms) in terms of the toroidal and poloidal components of  $\vec{\omega}$ .

**THEOREM 5.1.** *Let  $\lambda_\omega, \lambda_a, \gamma_\omega, \gamma_a$  be defined as in equations (4.2) and (4.3). The Navier–Stokes equations can be rewritten in the following way:*

$$(5.1) \quad \left( \frac{\partial}{\partial t} - \frac{1}{Re} \nabla^2 \right) \lambda_\omega = \lambda_a, \quad \left( \frac{\partial}{\partial t} - \frac{1}{Re} \nabla^2 \right) \gamma_\omega = \gamma_a.$$

*Proof.* The primitive form of the incompressible equation is as follows:

$$\left( \frac{\partial}{\partial t} + \vec{v} \cdot \nabla \right) \vec{v} = \frac{1}{Re} \nabla^2 \vec{v} - \nabla p,$$

with the additional constraint that  $\vec{v}$  is incompressible. Take the curl of both sides of the equation, noting that  $\nabla \times \nabla p = 0$  and that the curl commutes with univariate derivatives and the vector Laplacian, and substitute  $\vec{\omega} = \nabla \times \vec{v}$  where applicable:

$$\frac{\partial}{\partial t} \vec{\omega} + \nabla \times [\vec{v} \cdot \nabla \vec{v}] = \frac{1}{Re} \nabla^2 \vec{\omega}.$$

Using the identity  $\frac{1}{2} \nabla(\vec{V} \cdot \vec{V}) = (\vec{V} \cdot \nabla) \vec{V} + \vec{V} \times \nabla \times \vec{V}$ ,

$$\frac{\partial}{\partial t} \vec{\omega} - \nabla \times [\vec{v} \times \vec{\omega}] = \frac{1}{Re} \nabla^2 \vec{\omega}.$$

Now, substitute the PT decompositions in equations (4.2) and (4.3):

$$\begin{aligned} \frac{\partial}{\partial t} (\nabla \times [\lambda_\omega \hat{z}] + \nabla \times \nabla \times [\gamma_\omega \hat{z}]) - \frac{1}{Re} \nabla^2 (\nabla \times [\lambda_\omega \hat{z}] + \nabla \times \nabla \times [\gamma_\omega \hat{z}]) \\ = \nabla \times [\lambda_a \hat{z}] + \nabla \times \nabla \times [\gamma_a \hat{z}]. \end{aligned}$$

Commute the operators such that the curls are applied last:

$$\nabla \times \left[ \left( \frac{\partial}{\partial t} - \frac{1}{Re} \nabla^2 \right) \lambda_\omega \hat{z} \right] + \nabla \times \nabla \times \left[ \left( \frac{\partial}{\partial t} - \frac{1}{Re} \nabla^2 \right) \gamma_\omega \hat{z} \right] = \nabla \times [\lambda_a \hat{z}] + \nabla \times \nabla \times [\gamma_a \hat{z}].$$

The LHS and RHS of this equation represent two different PT decompositions of the same vector field. Because the poloidal and toroidal *vector fields* are unique, this

equation can be decoupled:

$$\begin{aligned}\nabla \times \left[ \left( \frac{\partial}{\partial t} - \frac{1}{Re} \nabla^2 \right) \lambda_\omega \hat{z} \right] &= \nabla \times [\lambda_a \hat{z}], \\ \nabla \times \nabla \times \left[ \left( \frac{\partial}{\partial t} - \frac{1}{Re} \nabla^2 \right) \gamma_\omega \hat{z} \right] &= \nabla \times \nabla \times [\gamma_a \hat{z}].\end{aligned}$$

Nonphysical gauge symmetries are available for each scalar component due to the presence of curls. Thus, these equations can be satisfied and these gauge symmetries removed by removing the curls and enforcing that the poloidal and toroidal scalars are the same on each side. Then we retrieve system (5.1). To show that a solution of this system uniquely determines  $\vec{v}$ , note that its PT decomposition *does* uniquely determine  $\vec{\omega}$ . From the Helmholtz Theorem [Zho06], specifying a vector field's curl and divergence (along with boundary conditions, as detailed in the appendix) uniquely determines that vector field. As  $\nabla \cdot \vec{v} = 0$  and  $\vec{\omega} \equiv \nabla \times \vec{v}$  is also known,  $\vec{v}$  is determined.  $\square$

Taking  $\lambda_\omega, \lambda_a, \gamma_\omega, \gamma_a$  all to be functions of time, our first step in solving the system (5.1) is to write these equations as matrix equations.

The  $m \times n$  matrix  $\mathbf{\Lambda}_{\omega, \ell}(t)$  [resp.  $\mathbf{\Gamma}_{\omega, \ell}(t)$ ] is defined by  $(\mathbf{\Lambda}_{\omega, \ell}(t))_{j, k} = \lambda_\omega^{(j, k, \ell)}$  [resp.  $(\mathbf{\Gamma}_{\omega, \ell}(t))_{j, k} = \gamma_\omega^{(j, k, \ell)}$ ], where  $(\lambda_\omega^{(j, k, \ell)})$  [resp.  $(\gamma_\omega^{(j, k, \ell)})$ ] are the interpolation coefficients for  $\lambda_\omega$  [resp.  $\gamma_\omega$ ] in CCF $_{(n, m, p)}$ . We define  $\mathbf{\Lambda}_{a, \ell}(t)$   $\mathbf{\Gamma}_{a, \ell}(t)$  the same way, but for  $\lambda_a$  and  $\gamma_a$ .

Initial conditions  $\mathbf{\Lambda}_{\omega, \ell}(0)$  and  $\mathbf{\Gamma}_{\omega, \ell}(0)$  can be found by replacing  $\vec{V}$  by  $\vec{\omega}(r, z, \theta, 0)$  in (4.4) and solving the discretized Poisson equations. The same can be said of  $\mathbf{\Lambda}_{a, \ell}(t)$  and  $\mathbf{\Gamma}_{a, \ell}(t)$ , once  $\nabla \times [\vec{v}(t) \times \vec{\omega}(t)]$  is known. To find  $\nabla \times [\vec{v}(t) \times \vec{\omega}(t)]$ , the following theorem is needed:

**THEOREM 5.2.** *Let  $\vec{\Psi}$  be the vector potential for  $\vec{v}$ ; that is,  $\vec{v} = \nabla \times \vec{\Psi}$ . If the PT decomposition of  $\vec{\Psi}$  is  $\vec{\Psi} = \nabla \times [\lambda_\psi \hat{z}] + \nabla \times \nabla \times [\gamma_\psi \hat{z}]$ , then the following is a decomposition of  $\vec{\omega} \equiv \nabla \times \vec{v}$ :*

$$\vec{\omega} = \nabla \times [-\nabla^2 \lambda_\psi \hat{z}] + \nabla \times \nabla \times [-\nabla^2 \gamma_\psi \hat{z}].$$

*Proof.* By taking two curls of the PT decomposition of  $\Psi$ , it is shown that  $\vec{\omega} = \nabla \times \nabla \times \nabla \times [\lambda_\psi \hat{z}] + \nabla \times \nabla \times \nabla \times \nabla \times [\gamma_\psi \hat{z}]$ . From the definition of a vector Laplacian,  $\nabla \times \nabla \times \vec{V} = \nabla[\nabla \cdot \vec{V}] - \nabla^2 \vec{V}$ . Under a curl, the gradient term vanishes. Then  $\nabla \times \nabla \times \nabla \times \vec{V} = \nabla \times [-\nabla^2 \vec{V}]$ . Applying this to both sides of the above equation retrieves our desired equality.  $\square$

Define  $\mathbf{\Gamma}_{\psi, \ell}(t)$  and  $\mathbf{\Lambda}_{\psi, \ell}(t)$  the same way we did  $\mathbf{\Lambda}_{\omega, \ell}(t)$  and  $\mathbf{\Gamma}_{\omega, \ell}(t)$ , but for  $\lambda_\psi$  and  $\gamma_\psi$ . We can find  $\lambda_\psi$  and  $\gamma_\psi$  at any time  $t$  using the following discretized Poisson

equations:

$$(RC_{12}D_1 + R^2D_2 - \ell^2C_{02})\mathbf{\Lambda}_{\psi,\ell}(t)C_{02}^T + R_2\mathbf{\Lambda}_{\psi,\ell}(t)D_2^T = -R_2\mathbf{\Lambda}_{\omega,\ell}C_{02}^T,$$

$$(RC_{12}D_1 + R^2D_2 - \ell^2C_{02})\mathbf{\Gamma}_{\psi,\ell}(t)C_{02}^T + R_2\mathbf{\Gamma}_{\psi,\ell}(t)D_2^T = -R_2\mathbf{\Gamma}_{\omega,\ell}C_{02}^T.$$

By taking appropriate curls,  $\vec{v}$  and  $\vec{\omega}$  can be recovered, and thus  $\nabla \times [\vec{v} \times \vec{\omega}]$  can be calculated directly:  $\vec{v} = \nabla \times [\gamma_\omega \hat{z}] + \nabla \times \nabla \times [\lambda_\psi \hat{z}]$  and  $\vec{\omega} = \nabla \times [\lambda_\omega \hat{z}] + \nabla \times \nabla \times [\gamma_\omega \hat{z}]$ . The first equality results from the fact that the curl of the toroidal field of  $\vec{A}$  is the poloidal field of  $\nabla \times \vec{A}$  for any incompressible  $\vec{A}$ . From here, we can write the Navier-Stokes equations as a system of discretized heat equations. The system (5.1) can be written as follows and solved using the ADI method:

$$\begin{aligned} \left( R_2 - \frac{\kappa^{(b)}}{Re} (RC_{12}D_1 + R^2D_2 - \ell^2C_{02}) \right) \mathbf{\Lambda}_{\omega,\ell}(t+h)C_{02}^T - \frac{\kappa^{(b)}}{Re} R_2 \mathbf{\Lambda}_{\omega,\ell}(t+h)D_2^T = \\ R_2 \left( \delta^{(b)} \mathbf{\Lambda}_{\omega,\ell}(t) + \kappa^{(b)} \mathbf{\Lambda}_{a,\ell}(t) \right) C_{02}^T, \\ \left( R_2 - \frac{\kappa^{(b)}}{Re} (RC_{12}D_1 + R^2D_2 - \ell^2C_{02}) \right) \mathbf{\Gamma}_{\omega,\ell}(t+h)C_{02}^T - \frac{\kappa^{(b)}}{Re} R_2 \mathbf{\Gamma}_{\omega,\ell}(t+h)D_2^T = \\ R_2 \left( \delta^{(b)} \mathbf{\Gamma}_{\omega,\ell}(t) + \kappa^{(b)} \mathbf{\Gamma}_{a,\ell}(t) \right) C_{02}^T. \end{aligned}$$

**6. Numerical Experiments.** Three methods for solving the forced heat equation were tested against an exact solution using various discretization sizes. Below are the maximum relative error values for these methods, as well as the computational times required to find these solutions. The first two methods were run for 200 time steps, with  $N = 7^3, 11^3, 15^3$ , and  $19^3$  in trials 1, 2, 3, and 4 respectively. Due to machine limitations, the finite difference method was only run for 6 time steps, with  $N = 61^3, 81^3, 101^3$ , and  $121^3$  respectively. The new spectral method achieves the highest accuracy in the least computational time of the tested methods.

Method \ Trial #	Maximum Error			
	1	2	3	4
New Spectral Method	$6.03 \cdot 10^{-5}$	$5.88 \cdot 10^{-5}$	$3.22 \cdot 10^{-5}$	$1.76 \cdot 10^{-5}$
Spectral Collocation	$6.40 \cdot 10^{-5}$	$5.85 \cdot 10^{-3}$	$3.51 \cdot 10^{-5}$	$5.90 \cdot 10^{-3}$
Finite Difference	$3.80 \cdot 10^{-1}$	$2.93 \cdot 10^{-1}$	$2.39 \cdot 10^{-1}$	$2.00 \cdot 10^{-1}$

Method \ Trial #	Computational Time (sec)			
	1	2	3	4
New Spectral Method	1.00	3.19	5.88	6.50
Spectral Collocation	1.06	4.42	11.9	17.9
Finite Difference	25.1	28.3	56.8	100

**7. Conclusion.** There are several published current methods which can be used to approximate solutions to the heat equation in a cylinder, but they share three major limitations: 1) They often either cluster points near the centerline of the cylinder or resolve the boundary only with linearly decaying error, 2) they have algebraically decaying errors over the whole cylinder, and 3) they have relatively high computational cost (often  $\mathcal{O}(N^{7/3})$  or higher).

The method described resolves all of these in turn. By choosing a “doubled” Chebyshev-Chebyshev-Fourier (CCF) discretization grid, it resolves all parts of the cylinder with high accuracy and without clustering discretization points. The algebraically decaying error associated with other methods is replaced with *spectral accuracy* by using high-degree polynomial interpolants to the velocity field over the whole cylinder. This accuracy generally represents an improvement of several orders of magnitude over previous methods, critical to our later application to the turbulence modeling. Finally, by leveraging the ADI method to solve the resulting equations in our CCF basis, our algorithm cuts the computational cost to  $\mathcal{O}(N \log N)$  operations (“near-optimal time”) per time step.

**Appendix: Boundary Conditions.** There are three sets of boundary conditions that need to be employed by our method. First, conditions for computing the PT decomposition of a given vector field. Second, conditions for finding the components of the vector potential of  $\vec{v}$ , as in Theorem 5.2. Finally, we need conditions for solving the discretized Navier–Stokes equations (5.1).

For the PT decomposition  $\vec{V} = \nabla \times [\lambda \hat{z}] + \nabla \times \nabla \times [\gamma \hat{z}]$  to be correct, it must satisfy one equality for each of the three vector components  $(\hat{r}, \hat{\theta}, \hat{z})$  of  $\vec{V}$ . Since the  $\hat{z}$  component is folded into the horizontal Poisson equation, we are left with  $\partial_\theta \lambda + r \partial_r \partial_z \gamma = r V^r$  and  $\partial_\theta \partial_z \gamma - r \partial_r \lambda = r V^\theta$ , where  $\vec{V} = V^r \hat{r} + V^\theta \hat{\theta} + V^z \hat{z}$ . These

equations only need to be enforced on the boundary of the cylinder, and can be discretized in the same manner as were the Helmholtz and Poisson equations.

In order to find the vector potential  $\vec{\Psi}$ , we use *no-slip* boundary conditions (though other conditions would work equally well)—that is, the boundary of the cylinder is non-moving and frictional. With that restriction, the vector potential is normal to the boundary of the cylinder (which can be seen from Stokes' Theorem). When  $z = \pm 1$ , the  $\hat{r}$  and  $\hat{\theta}$  components of  $\Psi$  must vanish:  $\partial_\theta \lambda_\psi + r \partial_r \partial_z \gamma_\psi = \partial_\theta \partial_z \gamma_\psi - r \partial_r \lambda_\psi = 0$ . When  $r = 1$ , the  $\hat{z}$  and  $\hat{\theta}$  components of  $\Psi$  must vanish:  $(r \partial_r + r^2 \partial_r^2 + \partial_\theta^2) \gamma_\psi = \partial_\theta \partial_z \gamma_\psi - r \partial_r \lambda_\psi = 0$ . These equations can be discretized as before.

For solving the Navier–Stokes equations, we continue to use no-slip conditions. Due to work by Quartepelle [QVG81], it is known that this no-slip condition on the velocity field is equivalent to the vorticity field being  $L^2$  orthogonal to all incompressible vector fields  $\vec{\eta}$  with  $\nabla^2 \vec{\eta} = 0$ . To form these  $\vec{\eta}$ , first let  $(\eta_i)$  be a basis of scalar cylindrical harmonics. For some  $i$ , let  $\vec{\eta}_i = \nabla \times [\eta_i \hat{z}]$  and  $\vec{\eta}_i^{(2)} = \nabla \times \nabla \times [\eta_i \hat{z}]$ . As all incompressible vector fields have a PT decomposition and the Laplacian commutes with the curl, the set  $\{\vec{\eta}_i\} \cup \{\vec{\eta}_i^{(2)}\}$  spans the set of  $\vec{\eta}$ . To achieve  $L^2$  orthogonality between  $\vec{\omega}$  and  $\vec{\eta}$  in  $C$ , the following equation must be met:

$$\begin{aligned} \int_C (\vec{\eta} \cdot (\nabla \times [\lambda_\omega \hat{z}] + \nabla \times \nabla \times [\gamma_\omega \hat{z}])) dV \\ = \int_C ([\nabla \times \vec{\eta}] \cdot \lambda_\omega \hat{z}) dV + \int_{\partial C} (\vec{n} \cdot [\lambda_\omega \hat{z} \times \vec{\eta}]) dS \\ + \int_{\partial C} (\vec{n} \cdot [\gamma_\omega \hat{z} \times \nabla \times \vec{\eta} + (\nabla \times \vec{\eta}) \times \gamma_\omega \hat{z}]) dS = 0. \end{aligned}$$

Let  $\vec{\eta} = \eta^r \hat{r} + \eta^\theta \hat{\theta} + \eta^z \hat{z}$ . Then the above equation simplifies to

$$\begin{aligned} \int_{r=1} \eta^\theta \lambda_\omega d\theta dz + \int_C [\eta^\theta + r \partial_r \eta^\theta - \partial_\theta \eta^r] \lambda_\omega dr d\theta dz \\ + \int_{r=1} ([\partial_z \eta^r - \partial_r \eta^z] \gamma_\omega + \eta^z \partial_r \gamma_\omega) d\theta dz \\ - \int_{z=1} (\eta^\theta \partial_\theta \gamma_\omega + r \eta^r \partial_r \gamma_\omega) dr d\theta \\ + \int_{z=-1} (\eta^\theta \partial_\theta \gamma_\omega + r \eta^r \partial_r \gamma_\omega) dr d\theta = 0. \end{aligned}$$

This equation can be discretized as before, creating one boundary condition for each  $\vec{\eta}$ . These conditions can also be included without “coupling in  $\theta$ ” by first enforcing a simpler set of boundary conditions and then performing a low-rank update on the solution matrix.



## REFERENCES

- [ARW95] Uri M. Ascher, Steven J. Ruuth, and Brian T. R. Wetton. Implicit-explicit methods for time-dependent partial differential equations. *SIAM Journal on Numerical Analysis*, 32(3):797–823, 1995.
- [BDST21] Nicolas Boullé, David Darrow, Jonasz Słomka, and Alex Townsend. An optimal complexity spectral method for navier–stokes simulations in the ball, 2021.
- [Ber09] Stefano Berrone. A local-in-space-timestep approach to a finite element discretization of the heat equation with a posteriori estimates. *SIAM Journal on Numerical Analysis*, 47(4):3109–3138, 2009.
- [Boy00] John Boyd. Chebyshev and fourier spectral methods. Oct. 2000.
- [BT07] Piotr Boronski and Laurette S. Tuckerman. Poloidal–toroidal decomposition in a finite cylinder. i: Influence matrices for the magnetohydrodynamic equations. *Journal of Computational Physics*, 227(2):1523–1543, dec 2007.
- [BT20] Nicolas Boullé and Alex Townsend. Computing with functions in the ball. *SIAM Journal on Scientific Computing*, 42(4):C169–C191, jan 2020.
- [BVO<sup>+</sup>20] Keaton J. Burns, Geoffrey M. Vasil, Jeffrey S. Oishi, Daniel Lecoanet, and Benjamin P. Brown. Dedalus: A flexible framework for numerical simulations with spectral methods. *Physical Review Research*, 2(2), apr 2020.
- [CCCS16] Matthew F. Causley, Hana Cho, Andrew J. Christlieb, and David C. Seal. Method of lines transpose: High order l-stable  $O(N)$  schemes for parabolic equations using successive convolution. *SIAM Journal on Numerical Analysis*, 54(3):1635–1652, 2016.
- [CH52] C. F. Curtiss and J. O. Hirschfelder. Integration of stiff equations. *Proceedings of the National Academy of Sciences of the United States of America*, 38(3):235–243, 1952.
- [Coo12] J.M. Cooper. *Introduction to Partial Differential Equations with MATLAB*. Applied and Numerical Harmonic Analysis. Birkhäuser Boston, 2012.
- [Dar17] David Darrow. Spectral heat equation solver. <https://github.com/ddarrow90/spectral-heat-equation>, 2017.
- [FT19] Daniel Fortunato and Alex Townsend. Fast Poisson solvers for spectral methods. *IMA Journal of Numerical Analysis*, 40(3):1994–2018, 11 2019.
- [Kra79] Theodor Krauthammer. Accuracy of the finite element method near a curved boundary. *Computers & Structures*, 10:921–929, 1979.
- [LeV07] Randall LeVeque. *Finite Difference Methods for Ordinary and Partial Differential Equations: Steady-State and Time-Dependent Problems (Classics in Applied Mathematics Classics in Applied Mathemat)*. Society for Industrial and Applied Mathematics, USA, 2007.
- [LS98] J.M. Lopez and Jie Shen. An efficient spectral-projection method for the navier–stokes equations in cylindrical geometries: I. axisymmetric cases. *Journal of Computational Physics*, 139(2):308–326, 1998.
- [OT13] Sheehan Olver and Alex Townsend. A fast and well-conditioned spectral method. *SIAM Review*, 55(3):462–489, 2013.
- [PR55] D. W. Peaceman and H. H. Rachford, Jr. The numerical solution of parabolic and elliptic differential equations. *Journal of the Society for Industrial and Applied Mathematics*, 3(1):28–41, 1955.
- [QVG81] L. Quartapelle and F. Valz-Gris. Projection conditions on the vorticity in viscous incompressible flows. *International Journal for Numerical Methods in Fluids*, 1(2):129–144, 1981.
- [She96] Jie Shen. On error estimates of the projection methods for the navier-stokes equations:

- Second-order schemes. *Mathematics of Computation*, 65(215):1039–1065, 1996.
- [SK21] Christoph Strössner and Daniel Kressner. Fast global spectral methods for three-dimensional partial differential equations, 2021.
- [TC99] David Torres and Evangelos Coutsias. Pseudospectral solution of the two-dimensional navier–stokes equations in a disk. *SIAM Journal on Scientific Computing*, 21:378–403, 08 1999.
- [Tre19] Lloyd N. Trefethen. *Approximation Theory and Approximation Practice, Extended Edition*. SIAM-Society for Industrial and Applied Mathematics, Philadelphia, PA, USA, 2019.
- [WTW17] Heather Wilber, Alex Townsend, and Grady B. Wright. Computing with functions in spherical and polar geometries ii. the disk. *SIAM Journal on Scientific Computing*, 39(3):C238–C262, 2017.
- [Zhi15] Yang Zhiyin. Large-eddy simulation: Past, present and the future. *Chinese Journal of Aeronautics*, 28(1):11–24, 2015.
- [Zho06] Xingling Zhou. On uniqueness theorem of a vector function. *Progress in Electromagnetics Research-pier*, 65:93–102, 2006.